Heart Rate Controller Design for Cardiac Pacemaker

Julia Nako and Costas Psychalinos
Physics Department, Electronics Laboratory
University of Patras
Rio Patras, Greece
up1061029@upnet.gr; cpsychal@upatras.gr

***Abstract*—A fractional-order controller design, which is suitable for implementing a cardiac pacemaker control system is introduced in this work. The main offered benefit, with regards to the corresponding convectional implementation, is the reduced passive and active component count. The provided simulation results confirm the aforementioned benefit and the performance of the proposed structure.**

***Index Terms*—fractional-order controllers, fractional-order impedances, curve-fitting based approximation, cardiac pacemaker systems**

I. Introduction

The employment of fractional-order controllers offers the capability of achieving more accurate shaping of the open-loop frequency response for fulfilling the imposed specifications on phase margin, settling time etc., than that offered by their conventional integer-order counterparts [1]–[4]. This is originated from the extra degrees of freedom, resulting from the variable (non-integer) order of the integration and differentiation stages of the controller. Significant research effort has been performed for developing fractional-order controllers structures through the utilization of the following general procedures: a) by substituting the integer-order capacitors of conventional controllers by suitable RC networks, which approximate the behavior of the corresponding fractional-order capacitors [5], and b) by approximating the transfer function of the controller using an integer-order rational transfer function, resulting from the employment of appropriate tools which approximate the fractional-order Laplacian operator [6], [7]. The first one is an easy procedure, in the sense that just only one design step is required for deriving the structure of the fractional-order controller.

A simple general structure for implementing fractional-order proportional-integral-derivative ($\mathrm{PI}^{\lambda}\mathrm{D}^{\mu}$) controllers is presented in this work, which is based on the first one of the aforementioned procedures. The transfer function of the controller is expressed as ratio of an integer and a non-integer impedance, and the magnitude and phase frequency characteristics of the fractional-order impedance are approximated through the utilization of a curve-fitting based approximation tool. The paper is organized as follows: the conventional implementation is presented in Section II, while the proposed one is introduced in Section III. The behavior of the proposed controller, as well as of the controller-plant system, are evaluated through simulation results in Section IV.

979-8-3503-9958-5/22/$31.00

II. Proportional Integral Derivative Controller for Cardiac Pacemaker

Assuming that $0 < \lambda < 1$ and $0 < \mu < 1$ are the orders of the integration and differentiation stages, with K_i and K_d being their associated constants, then the transfer function of a $\mathrm{PI}^{\lambda}\mathrm{D}^{\mu}$ controller is given by (1)

$$C(s) = Kp + \frac{K_i}{s^{\lambda}} + K_d s^{\mu}\,, \tag{1}$$

with K_p being the constant associated with the proportional stage.
Using Current Feedback Operational Amplifiers (CFOAs) as active elements, a possible implementation of the transfer function in (1) is depicted in Fig. 1.

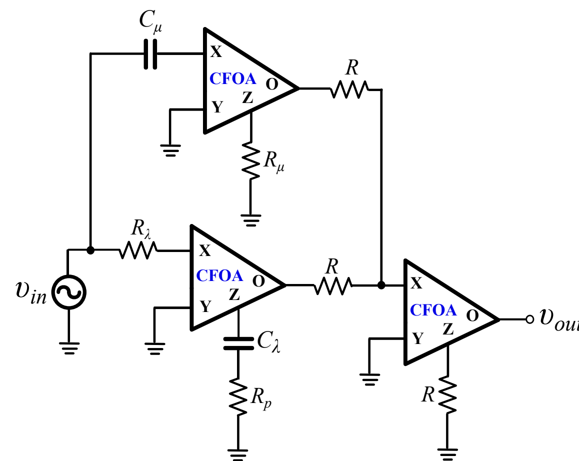

Fig. 1. Implementation of a $\mathrm{PI}^{\lambda}\mathrm{D}^{\mu}$ controller using CFOAs as active elements.

Taking into account the properties of the terminals of the CFOA given by the following formulas: $\upsilon_Y = \upsilon_X, \upsilon_O = \upsilon_Z, i_Z = i_X$, and $i_Y = 0$, as well as that the impedance of fractional-order capacitor of order $0 < a < 1$ and pseudo-capacitance C_α (in $F/s^{1-\alpha}$) is given by the expression: $Z = 1/C_\alpha s^{\alpha}$, it is obtained that this topology implements the transfer function:

$$H(S) = \frac{R_p}{R_\lambda} + \frac{1}{R_\lambda C_\lambda s^{\lambda}} + R_\mu C_\mu s^{\mu}\,. \tag{2}$$

Comparing (1)–(2) the following design equations are derived:

$$K_p = \frac{R_p}{R_\lambda},\quad K_i = \frac{1}{R_\lambda C_\lambda},\quad K_d = R_\mu C_\mu\,. \tag{3}$$

The approximation of the behavior of the fractional-order capacitors in Fig. 1 can be performed through the utilization of appropriately configured Foster or Cauer RC networks. Following this and choosing among a variety of approximation tools, such as the Oustaloup, Matsouda, continued fraction expansion etc., the expression of the impedance of a fractional-order capacitor is approximated by a n^{th}-order rational integer-order impedance function of the form:

$$Z_{approx}(s) = R\frac{B_n s^n + B_{n-1}s^{n-1} + \ldots + B_1 s + B_0}{s^n + A_{n-1}s^{n-1} + \ldots + A_1 s + A_0}, \tag{4}$$

with A_i and $B_i\,(i = 0\ldots n)$ being positive and real coefficients and R being an arbitrary resistance. The impedance function in (4) can be implemented by the Foster type-I network in Fig. 2 and the associated design equations are summarized in (5)

$$R_0 = RB_n \qquad R_i = R\frac{r_i}{|p_i|} \qquad C_i = R\frac{1}{r_i},\ \ (i = 1, 2...n), \tag{5}$$

with r_i and p_i being the residues and poles of (4) [8].

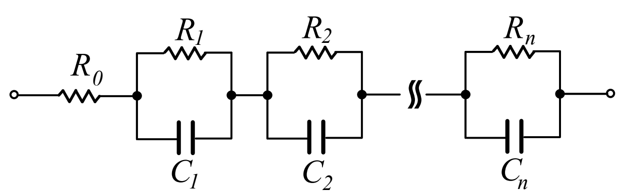

Fig. 2. Foster type-I RC network for approximating the behavior of fractional-order impedances.

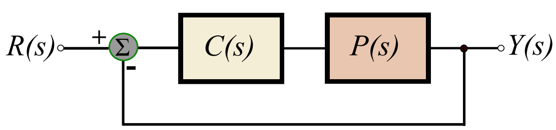

Fig. 3. Block diagram of the closed-loop system for the cardiac pacemaker.

Let us consider for example the closed-loop system of the cardiac pacemaker demonstrated in Fig. 3, where $C(s)$ is the transfer function of the controller, $P(s)$ is the product of the transfer functions which describe the dynamics of the pacemaker and the heart [9]–[11]. These are given by the expressions in (6)–(7)

$$C(s) = 0.72594 + \frac{0.1}{s^{0.01}} + 0.1s^{0.9786}, \tag{6}$$

$$P(s) = \frac{1352}{s(s+20.8)(s+8)}. \tag{7}$$

Also, $R(s)$ is the actual heart rate, while $Y(s)$ is the desired heart rate.

Assuming that $R_\lambda = 10M\Omega$ and $R_\mu = 100k\Omega$ the values of the pseudo-capacitances calculated using (3) are: $C_\lambda = 1\mu F/s^{0.99}$ and $C_\mu = 1\mu F/s^{0.0214}$. Utilizing a 3$^{\text{rd}}$–order Oustaloup approximation in the range [10^{-1},10^{2}]rad/s, then

TABLE I
PASSIVE ELEMENTS VALUES FOR APPROXIMATING THE FRACTIONAL-ORDER CAPACITORS IN FIG. 1.

Element	**Value**	
	$C_\lambda = 1\mu F/s^{0.99}$	$C_\mu = 1\mu F/s^{0.0214}$
R_0	931 $k\Omega$	1.15 $k\Omega$
R_1	36.5 $k\Omega$	3.83 $k\Omega$
R_2	38.3 $k\Omega$	169 $k\Omega$
R_3	39.2 $k\Omega$	90.9 $M\Omega$
C_1	191 nF	11.5 μF
C_2	8.45 μF	12.1 μF
C_3	383 μF	1.07 μF

the values of passive elements of the network in Fig. 2 calculated using (5), rounded to the E96 series defined in IEC 60063, are summarized in Table I.

III. Proposed Implementation of the Controller

In order to overcome the obstacle of the increased number of active and passive component count, an alternative topology for realizing the transfer in (1) is introduced in this paper, and is demonstrated in Fig. 4. The realized transfer function is

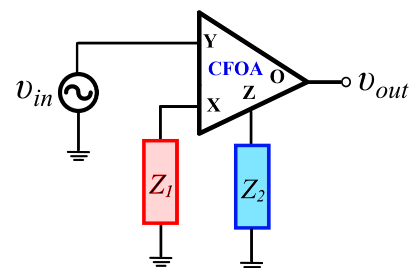

Fig. 4. CFOA based proposed topology for implementing the transfer function of a PI$^\lambda$D$^\mu$ controller.

given by (8)

$$H(s) = \frac{Z_2}{Z_1}, \tag{8}$$

where $Z_1 = R$ and $Z_2 = RC(s)$ or $Z_1 = R/C(s)$ and $Z_2 = R$, with R being a resistance of arbitrary value. The choice of the impedance which will have a fractional-order form depends on the behavior of the controller transfer function at high frequencies. More specifically, Z_2 will be fractional in the case of capacitive behavior (i.e., the gain is monotonically increased), while the opposite holds in the case of inductive behavior. The last one is the case of the controller described by (1) and, therefore $Z_1 = 1/RC(s)$ and $Z_2 = R$. The approximation of Z_1 will be performed using the Sanathanan-Koerner (SK) least square iterative method based on the following steps [12].

- Obtain the frequency response data of Z_1, within the desired frequency range, using the MATLAB *freqresp* and *frd* functions.
- Assuming an approximation order, obtain the state-space model of the data using the command *fitfrd*, and then convert this model to a transfer function using the MATLAB command *ss2tf*.

TABLE II
PASSIVE ELEMENTS VALUES FOR APPROXIMATING THE FRACTIONAL-ORDER IMPEDANCE IN FIG. 4

Element	Value
R_0	15.8 Ω
R_1	187 Ω
R_2	10.7 $k\Omega$
R_3	1.24 $k\Omega$
C_1	127 μF
C_2	10.2 μF
C_3	174 μF

TABLE III
COMPARISON OF THE THEORETICAL AND APPROXIMATED OPEN AND CLOSED-LOOP PERFORMANCES OF THE SYSTEM IN FIG. 3

Parameter	Value	
	Theoretical	Approximation
Phase margin (^{o})	70.39	70.34
Gain crossover frequency (rad/s)	6.34	6.34
Rise time (ms)	308.1	236.4
Settling time (ms)	472.7	355.4

The obtained impedance transfer function will have the form of (4) and, therefore, it is realizable by the topology in Fig. 2.

Following the aforementioned steps and considering the same frequency range of interest as well as the same order of approximation with in the previous case, the values of the passive element of the RC network calculated using (5) and assuming that $R = 10k\Omega$ are summarized in Table II.
The efficiency of the presented approximation is evaluated at transfer function level through the MATLAB software and the results are provided in Table III, where it is evident that a satisfactory accuracy is achieved.

With regards to the achieved reduced circuit complexity, the results of comparison are provided in Table IV, where they are obvious the benefits offered by the proposed scheme.

IV. SIMULATION RESULTS

The behavior of the system will be evaluated using the OrCAD PSpice simulator and the corresponding model of the AD844 discrete component IC, which will be employed as CFOA. The magnitude and phase frequency responses of the controller are provided in Fig. 5, with the corresponding theoretically predicted ones given by dashes, confirming the accurate operation of the introduced scheme of the controller.

The responses of the controller-plant system are demonstrated in Fig. 6. The closed-loop behavior of the system

TABLE IV
COMPARISON RESULTS OF THE CIRCUIT COMPLEXITY FOR THE TOPOLOGIES IN FIGS. 1 AND 4

Parameter	Value	
	Conventional (Fig. 1)	Proposed (Fig. 4)
Number of CFOAs	3	1
Number of resistors	14	5
Number of capacitors	6	3
Matching requirement	YES	NO

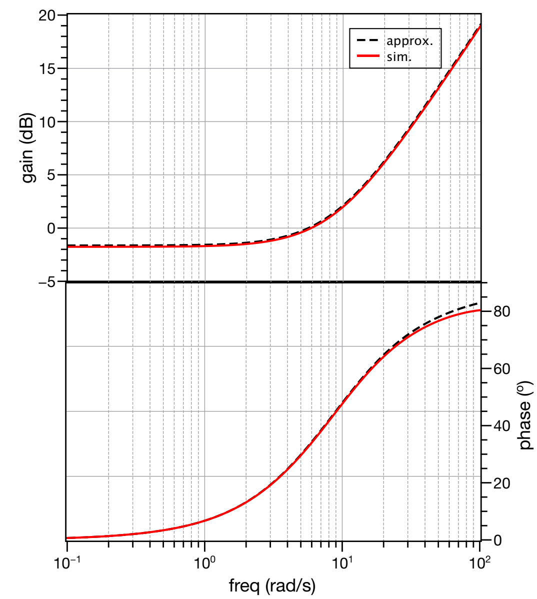

Fig. 5. Simulated gain and phase responses of the proposed controller.

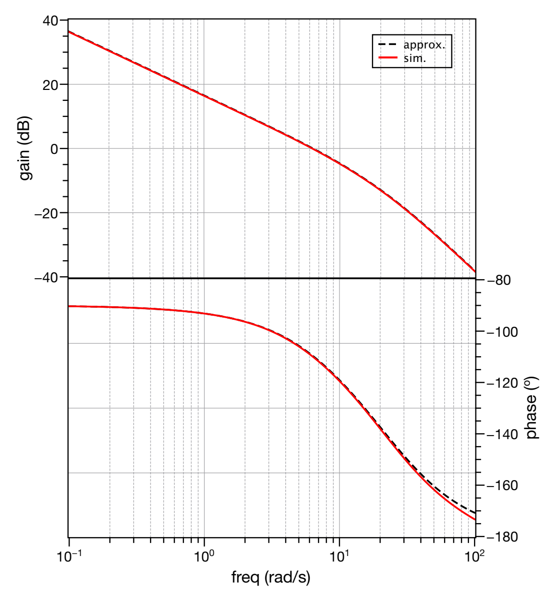

Fig. 6. Open-loop transfer function gain and phase responses of the system controller-plant.

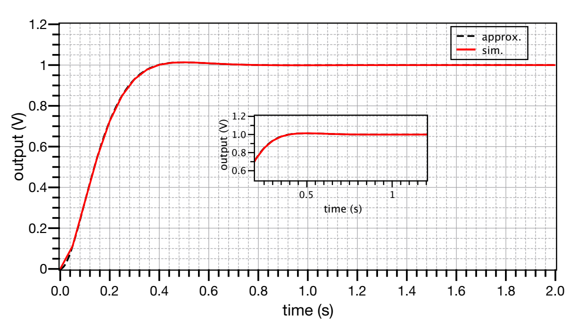

Fig. 7. Step response of the system controller-plant.

TABLE V
SIMULATION RESULTS OF THE SYSTEM IN FIG. 3

Parameter	Value	
	Approximation	Simulation
Phase margin (^{o})	70.34	70.31
Gain crossover frequency (rad/s)	6.34	6.25
Rise time (ms)	236.4	236.2
Settling time (ms)	355.4	393.23

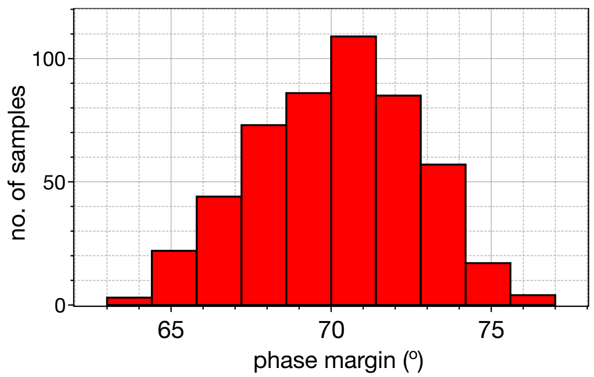

Fig. 8. Monte-Carlo analysis results of the phase margin of the control system.

is evaluated by stimulating it by a step voltage and the derived output waveform is provided in Fig. 7. The derived performance simulation results for both open-loop and closed-loop configuration are given in Table V, where it is readily obtained that the system behaves in a satisfactory level of accuracy.

The sensitivity of the system is evaluated using the Monte-Carlo analysis tool offered by the Advanced Analysis tool of the OrCAD PSpice suite, for N=500 runs and 10% random tolerances of the passive elements values.

The obtained statistical plots of the phase margin and gain crossover frequency are demonstrated in Figs. 8–9, where the associated values of the standard deviation are 2.5^o and $0.38 rad/s$. Taking into account that the corresponding nominal values are 70.31^o and $6.25 rad/s$, it is concluded that the proposed implementation offers reasonable sensitivity characteristics.

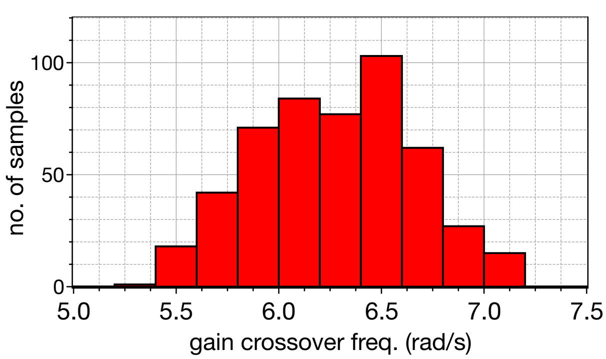

Fig. 9. Monte-Carlo analysis results of the gain crossover frequency of the control system.

V. CONCLUSIONS

The general topology for implementing fractional-order controllers, which is introduced in this work, offers design versatility and flexibility because the transfer function of the controller is considered, instead of the transfer functions of the intermediate stages. Thanks to this concept, structures with minimized circuit complexity are derived.

It must be also mentioned at this point that the presented procedure is general, in the sense that it can be utilized for realizing various types of non-integer controllers, filters, oscillators etc. [13], [14]. Exploitation of relevant electronically adjustable structures is the subject of ongoing research.

REFERENCES

[1] C. A. Monje, Y. Chen, B. M. Vinagre, D. Xue, and V. Feliu-Batlle, *Fractional-order systems and controls: fundamentals and applications*. Springer Science & Business Media, 2010.

[2] A. A. Dastjerdi, B. M. Vinagre, Y. Chen, and S. H. HosseinNia, "Linear fractional order controllers; a survey in the frequency domain," *Annual Reviews in Control*, vol. 47, pp. 51–70, 2019.

[3] W. Bauer and J. Baranowski, "Fractional PI$^\lambda$D controller design for a magnetic levitation system," *Electronics*, vol. 9, no. 12, p. 2135, 2020.

[4] A. Tepljakov, B. B. Alagoz, C. Yeroglu, E. A. Gonzalez, S. H. Hosseinnia, E. Petlenkov, A. Ates, and M. Cech, "Towards industrialization of fopid controllers: A survey on milestones of fractional-order control and pathways for future developments," *IEEE Access*, vol. 9, pp. 21 016–21 042, 2021.

[5] O. Domansky, R. Sotner, L. Langhammer, J. Jerabek, C. Psychalinos, and G. Tsirimokou, "Practical design of rc approximants of constant phase elements and their implementation in fractional-order pid regulators using cmos voltage differencing current conveyors," *Circuits, Systems, and Signal Processing*, vol. 38, no. 4, pp. 1520–1546, 2019.

[6] I. Dimeas, I. Petras, and C. Psychalinos, "New analog implementation technique for fractional-order controller: A DC motor control," *AEU-International Journal of Electronics and Communications*, vol. 78, pp. 192–200, 2017.

[7] C. Psychalinos, *Development of fractional-order analog integrated controllers-applications examples*. De Gruyter, 2019, pp. 357–378. [Online]. Available: https://doi.org/10.1515/9783110571745-016

[8] G. Tsirimokou, "A systematic procedure for deriving RC networks of fractional-order elements emulators using Matlab," *AEU-International Journal of Electronics and Communications*, vol. 78, pp. 7–14, 2017.

[9] S. P. Arunachalam, S. Kapa, S. K. Mulpuru, P. A. Friedman, and E. G. Tolkacheva, "Intelligent fractional-order PID (FOPID) heart rate controller for cardiac pacemaker," in *2016 IEEE Healthcare Innovation Point-Of-Care Technologies Conference (HI-POCT)*. IEEE, 2016, pp. 105–108.

[10] S. Bajpai, M. Alam, and M. Ali, "Intelligent heart rate controller using fractional order pid controller tuned by genetic algorithm for pacemaker," *International Journal of Engineering Research & Technology*, vol. 6, no. 5, pp. 715–720, 2017.

[11] S. Momani, I. M. Batiha, and R. El-Khazali, "Design of PI$^\lambda$D$^\delta$-heart rate controllers for cardiac pacemaker," in *2019 IEEE International Symposium on Signal Processing and Information Technology (ISSPIT)*. IEEE, 2019, pp. 1–5.

[12] K. Bingi, R. Ibrahim, M. N. Karsiti, S. M. Hassam, and V. R. Harindran, "Frequency response based curve fitting approximation of fractional-order pid controllers," *International Journal of Applied Mathematics and Computer Science*, vol. 29, no. 2, 2019.

[13] S. Kapoulea, C. Psychalinos, and A. S. Elwakil, "Reduced active element power-law proportional-integral controller designs," in *2021 3rd Novel Intelligent and Leading Emerging Sciences Conference (NILES)*. IEEE, 2021, pp. 51–54.

[14] ——, "Double exponent fractional-order filters: Approximation methods and realization," *Circuits, Systems, and Signal Processing*, vol. 40, no. 2, pp. 993–1004, 2021.